Supplementary Information

Lung-targeted feedback regulation of the mitochondrial ATP synthetic pathway for orthotopic tumors suppression

Zhou Jiang,[a] Songlan Pan,[c] Jianhua Chen,[a] Huihuang Yi,[a] Yingfeng Li,[b] Yi Qing,[a] Erhu Xiong*,[b] and Zhen Zou*,[b,c]

[a]Department of Thoracic Medicine, Affiliated Cancer Hospital of Xiangya School of Medicine, Hunan Cancer Hospital, Central South University, Changsha 410006, China

[b]Key Laboratory of Chemical Biology & Traditional Chinese Medicine Research Ministry of Education, Institute of Interdisciplinary Studies, College of Chemistry and Chemical Engineering, Hunan Normal University, Changsha 410081, China

[c]School of Chemistry and Chemical Engineering, Hunan Provincial Key Laboratory of Cytochemistry, Changsha University of Science and Technology, Changsha 410114, China

E-mails: xiongerhu2008@163.com; zouzhen2022@hunnu.edu.cn

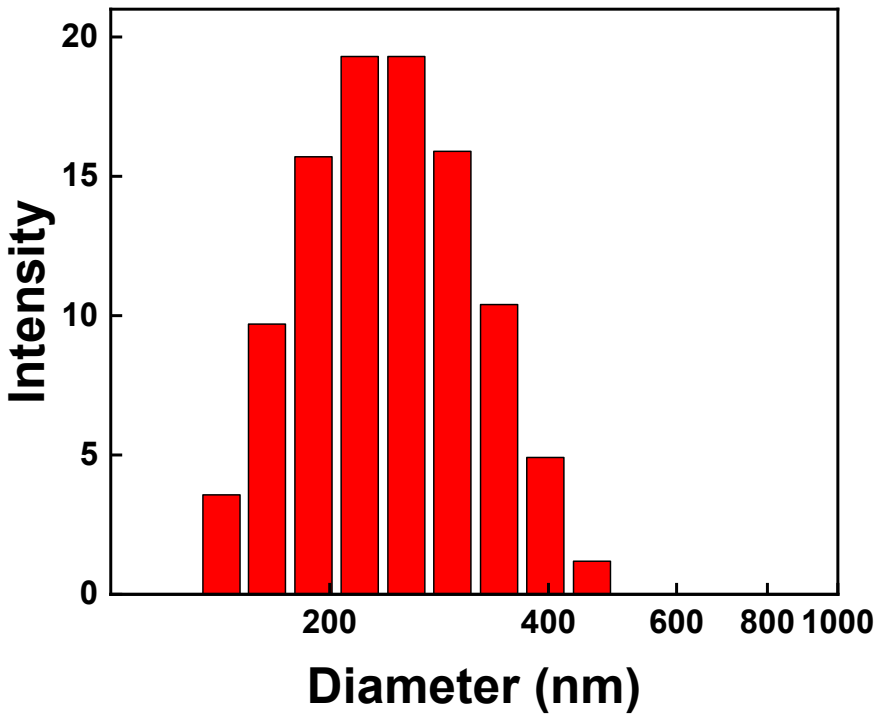

Fig. S1 Hydrodynamic diameter of ZIF-90/AIPH/BE.

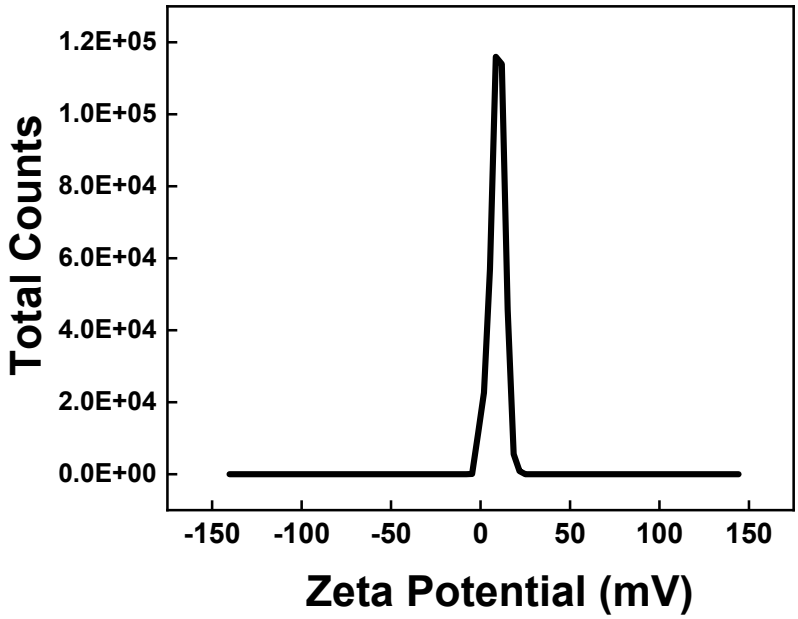

Fig. S2 Zeta potential diagram of ZIF-90/AIPH/BE.

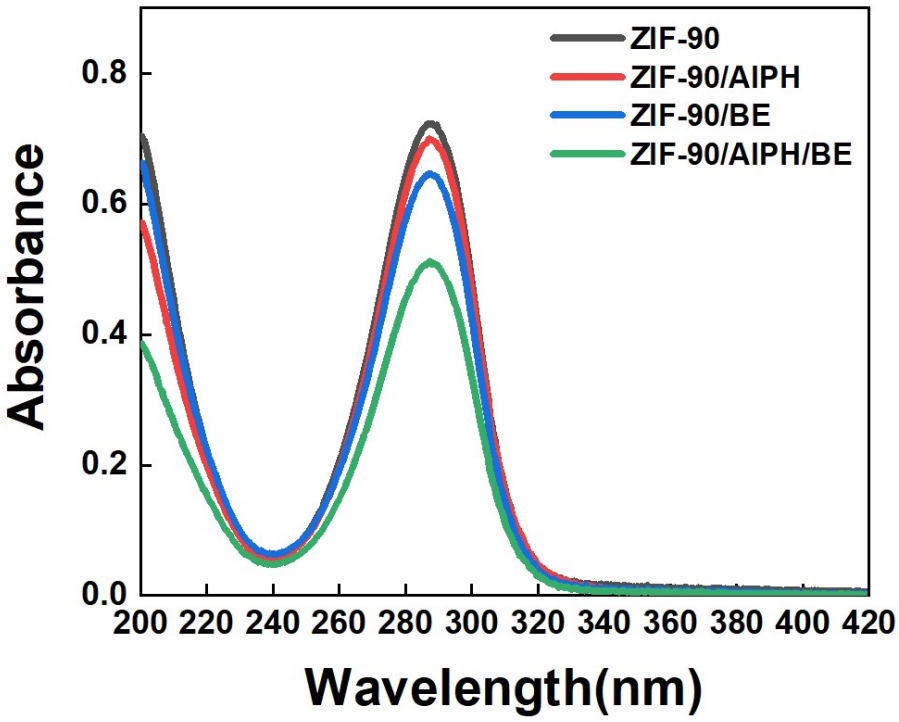

Fig. S3 UV spectra of ZIF-90, ZIF-90/AIPH, ZIF-90/BE, ZIF-90/AIPH/BE.

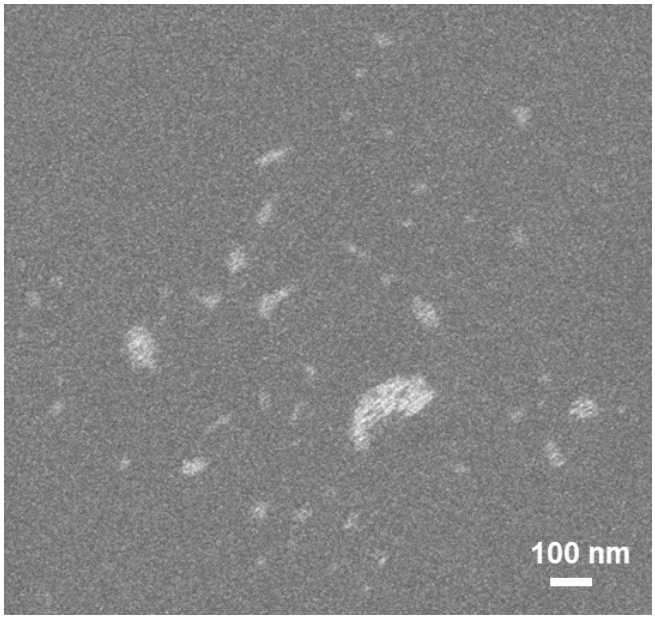

Fig. S4 SEM of ZIF-90/AIPH/BE after incubation with 2 mM ATP.

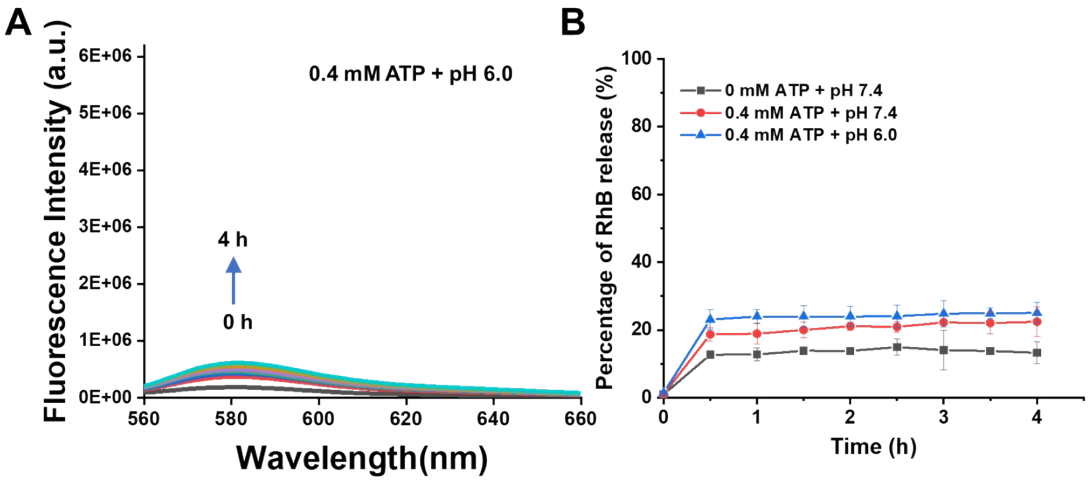

Fig. S5 Release profiles of RhB when subjected to the mimic extratumoral conditions: (A) the fluorescence spectra; (B) the amount of released RhB.

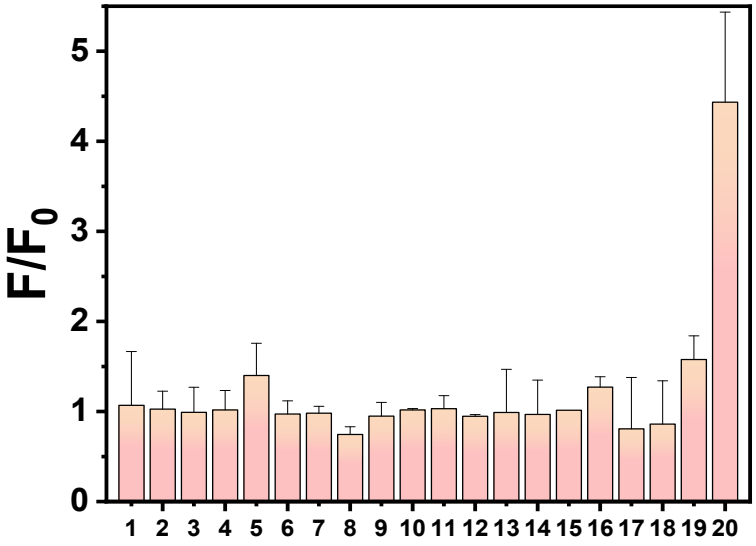

Fig. S6 The selectivity of ZIF-90/RhB nanoprobe for ATP. (1: K^+; 2: Na^+; 3: Ca^{2+}; 4: Mg^{2+}; 5: Cu^{2+}; 6: Ba^{2+}; 7: NH_4^+; 8: NO_3^-; 9: PO_3^{3-}; 10: SO_4^{2-}; 11: SO_3^{2-}; 12: CO_3^{2-}; 13: HCO^{3-}; 14: Br^-; 15: Cl^-; 16: Gly; 17: Glu; 18: GMP; 19: AMP; 20: ATP).

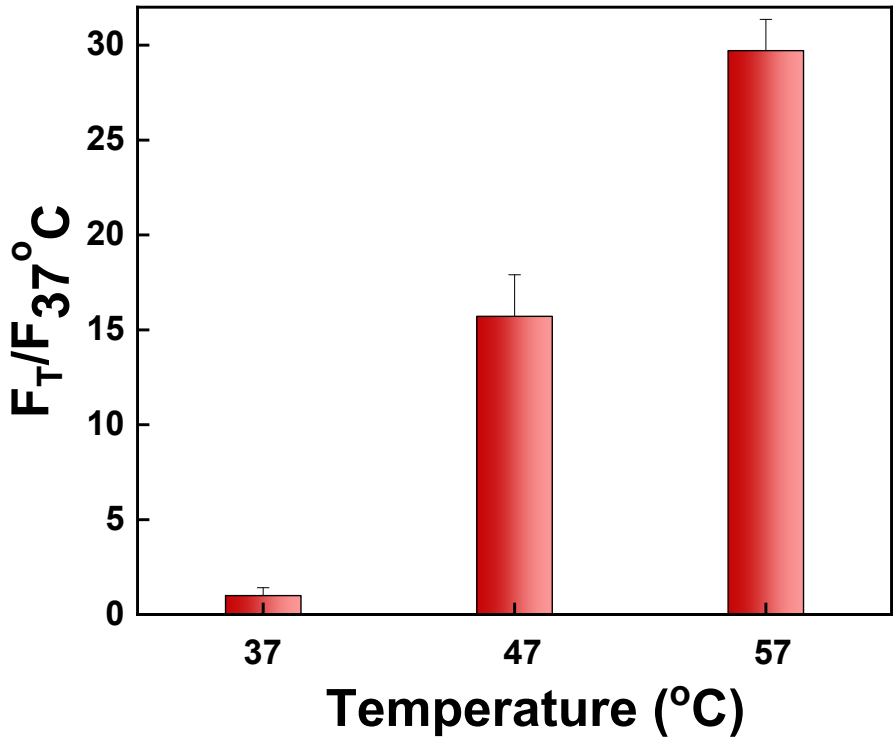

Fig. S7 Fluorescence ratio of DCF through a reaction between DCFH-DA and alkyl radicals from AIPH at different temperature.

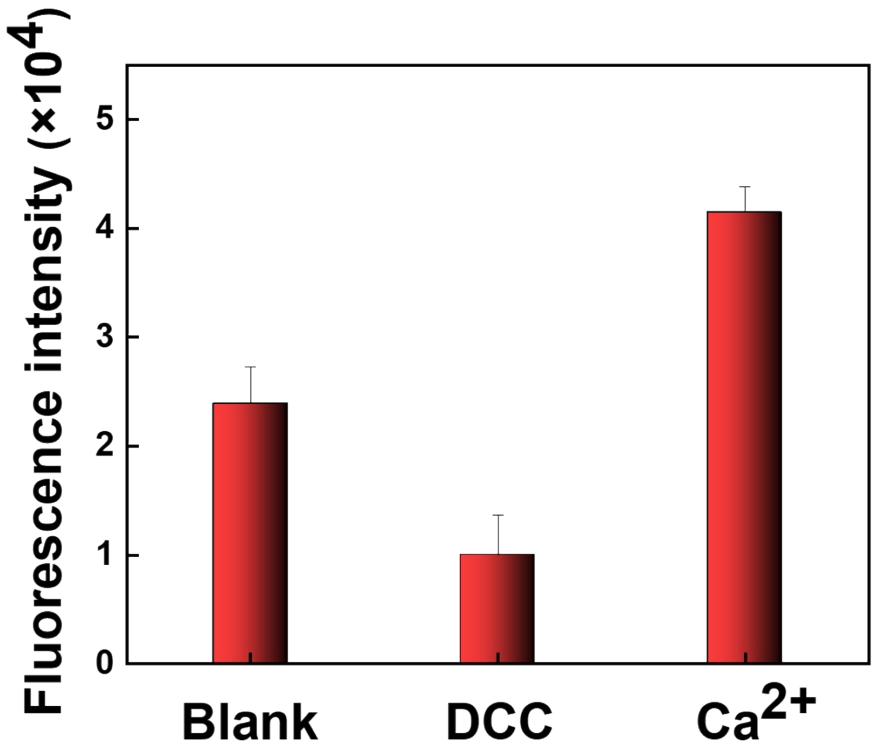

Fig. S8 Fluorescence intensity of ZIF-90/RhB in A549 cells upon treatment with DCC and Ca^{2+}.

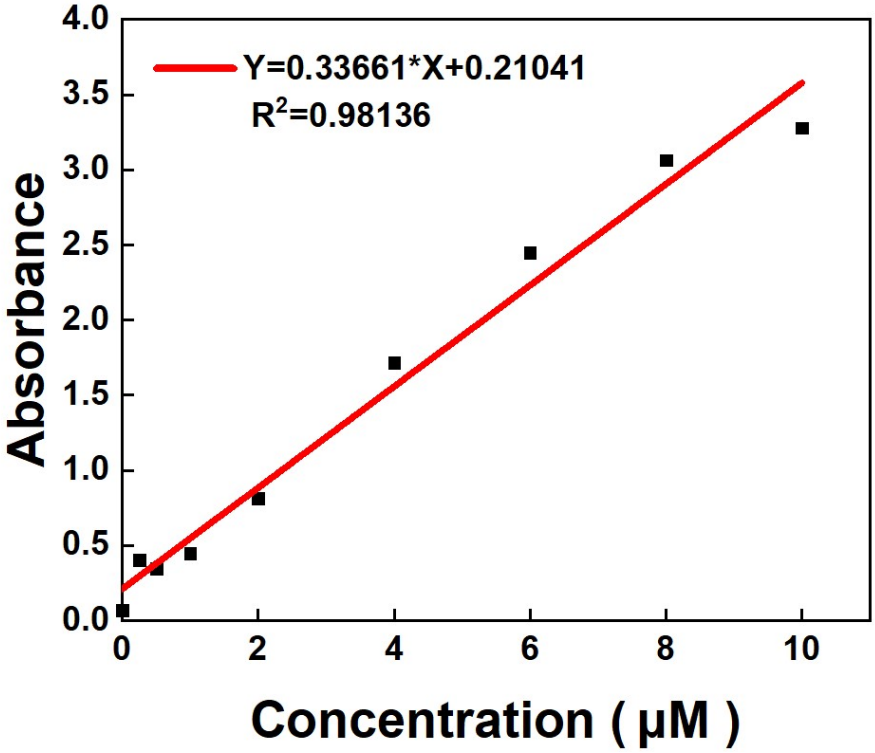

Fig. S9 Standard curve of NADH concentrations detected by Amplite Colorimetric Total NAD and NADH Assay Kit.

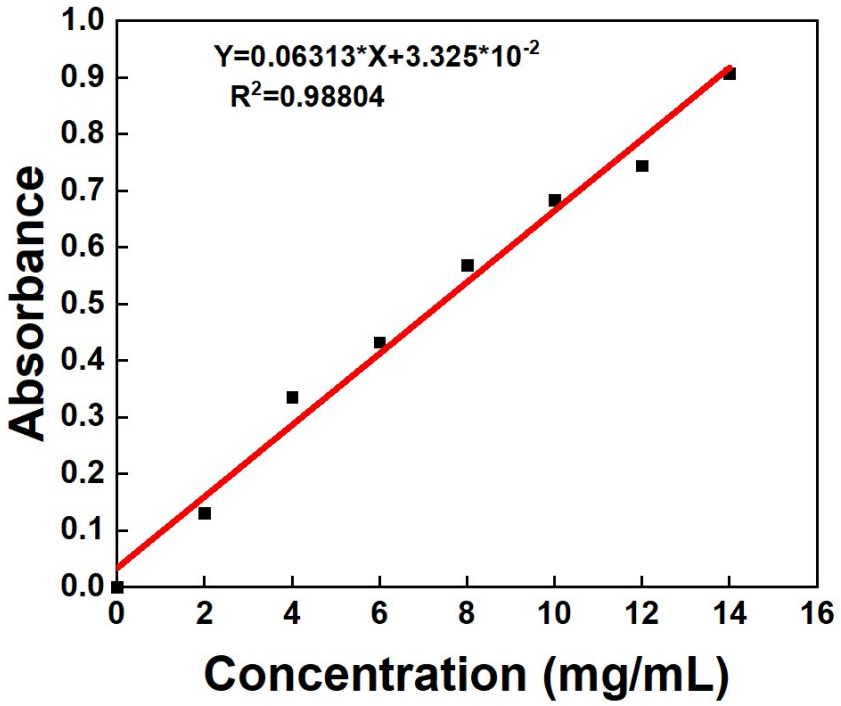

Fig. S10 Standard curve of ATP contents in A549 cells detected by ATP assay Kit.

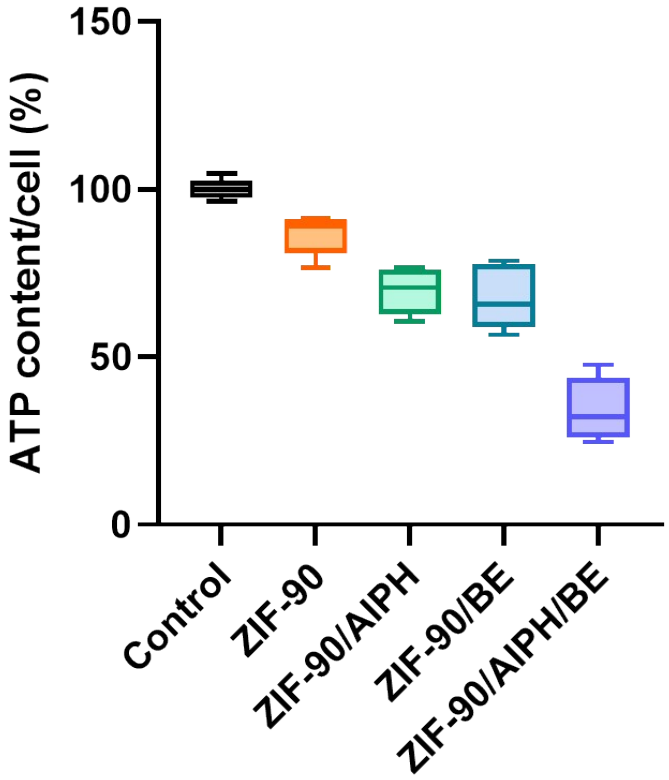

Fig. S11 ATP content in per cell after A549 cells were treated with different formulations for 24 h. The values of the control group were all set as 100%.

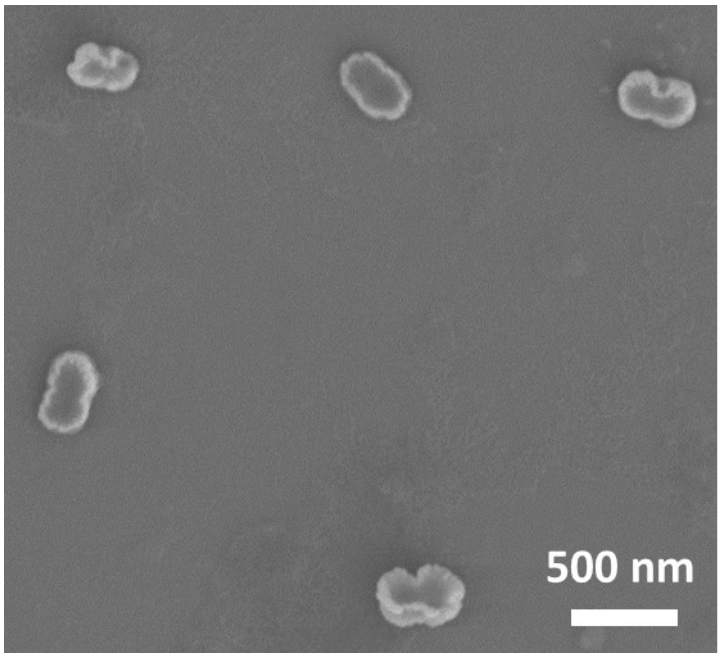

Fig. S12 SEM of mitochondrion-orientated liposome.

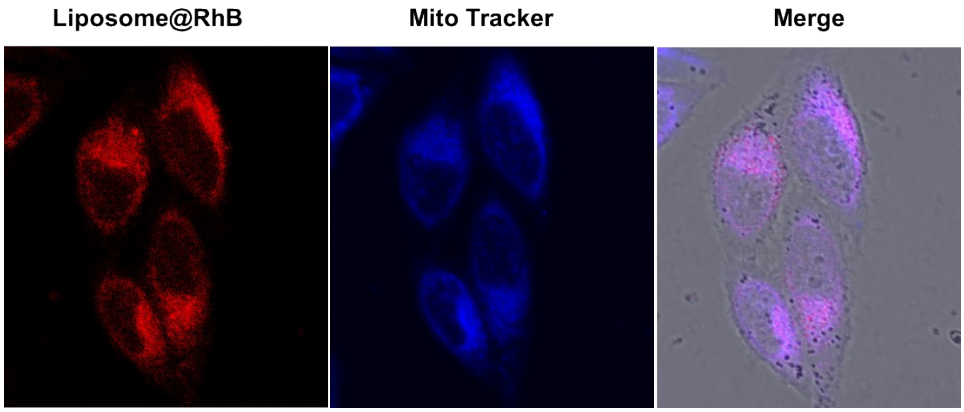

Fig. S13 Co-localization experiments involving mitochondrion-orientated liposome@RhB, MitoTracker in A549 cells.

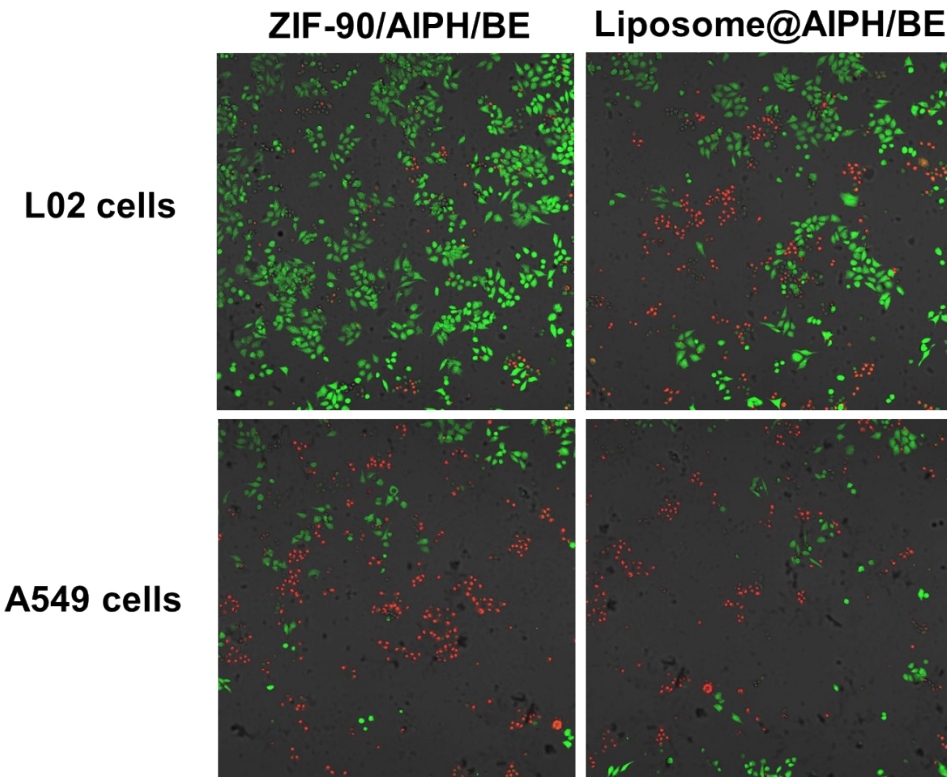

Fig. S14 AM/PI staining confocal microscopy images of A549 or LO2 cells with different treatments.

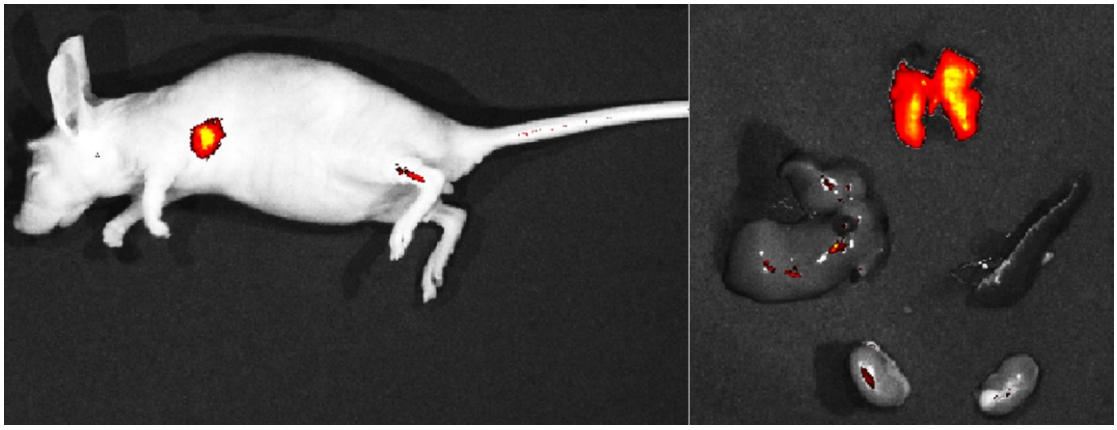

Fig. S15 *In vivo and ex vivo* fluorescence imaging after ZIF-90/Cy5.5 NPs was induced in normal Balb/c mice by intravenous injection for 2 h.

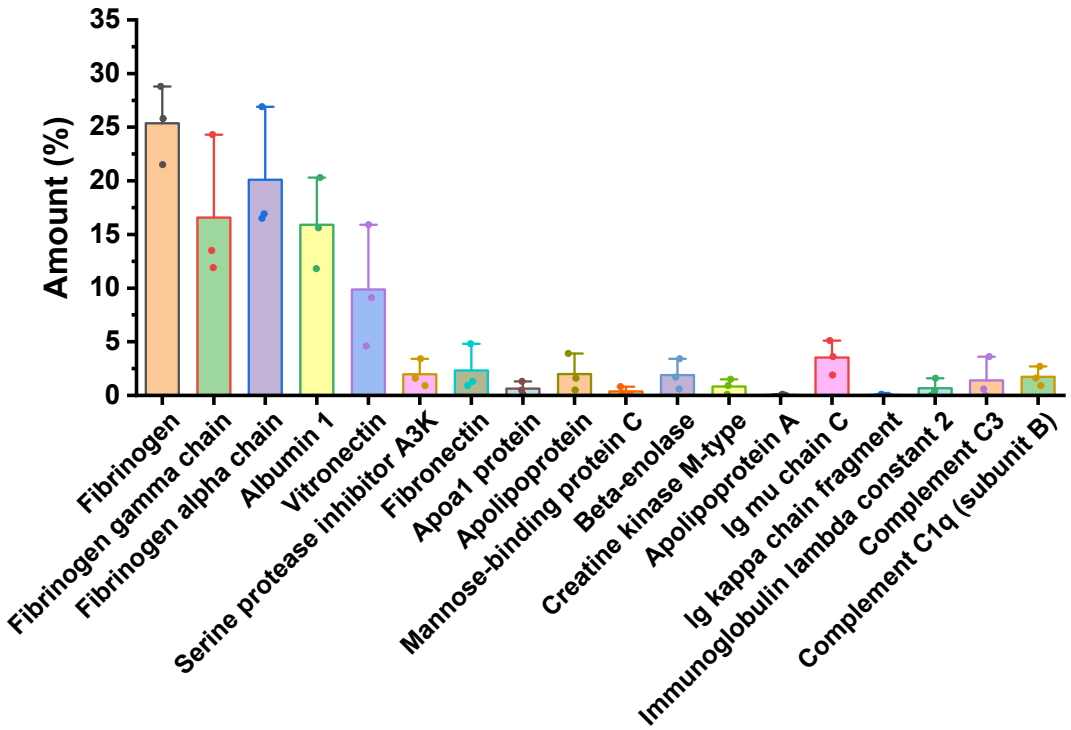

Fig. S16 The top 18 most abundant proteins in the protein corona of different nanoparticles determined. Values were calculated from the molar masses of each protein identified by LC–MS.